Publication II

Ilkka Laakso and Tero Uusitupa. 2008. Alternative approach for modeling material interfaces in FDTD. Microwave and Optical Technology Letters, volume 50, number 5, pages 1211-1214.

# ALTERNATIVE APPROACH FOR MODELING MATERIAL INTERFACES IN FDTD

**Ilkka Laakso and Tero Uusitupa**
Electromagnetics Laboratory, Helsinki University of Technology, Finland; Corresponding author: ilkka.laakso@tkk.fi

*Received 21 September 2007*

**ABSTRACT:** *A simple alternative way to position dielectric materials in the finite-difference time-domain (FDTD) Yee cell grid is proposed. Plane-wave illuminated spheres are used as examples to study the performance of the alternative method compared to the standard FDTD method. Although the performances are generally equally good, the alternative method may sometimes give significantly improved accuracy.* © 2008 Wiley Periodicals, Inc. Microwave Opt Technol Lett 50: 1211–1214, 2008; Published online in Wiley InterScience (www.interscience.wiley.com). DOI 10.1002/mop.23309

**Key words:** *finite-difference time-domain (FDTD) method; dielectric discontinuities*

## 1. INTRODUCTION

The finite-difference time-domain (FDTD) method, for example, [1, 2], is a popular tool for numerically solving electromagnetic problems by finite-difference approximation of Maxwell's equations. FDTD has a wide range of applications, many of which include modeling dielectric or magnetic materials. In this letter, an alternative method for including dielectric materials in the FDTD staircase grid is proposed. Numerical examples, which illustrate that the alternative method may prove advantageous in some problems, are presented. In the following, nonmagnetic materials are assumed for simplicity.

## 2. POSITIONING MATERIALS IN FDTD GRID

In the standard FDTD method, the material cells are positioned in the E-cell grid (see Fig. 1). In such grid, modeling solid dielectric objects is done using the staircase approximation, that is, the material parameters $\varepsilon$ and $\sigma$ are assumed piecewise constant, such that the material is constant inside a single Yee cell. The electric field components are located on the E-cell edges, which automatically enforces the continuity of tangential electric field across dielectric interfaces.

Tangential component of the electric flux density is needed for the FDTD update equations, yet it is undefined on material interfaces in a physical sense. Solution is to introduce an effective electric flux density, which is a linear average of the physical electric flux densities of the four neighboring cells (see Fig. 2). The effective electric flux density and the electric field are linked by the effective permittivity, which is

$$\varepsilon_{\text{eff}} = \frac{1}{4}(\varepsilon_1 + \varepsilon_2 + \varepsilon_3 + \varepsilon_4), \tag{1}$$

using the notation from Figure 2. Similarly, by introducing effective current density, the effective conductivity on the edge is

$$\sigma_{\text{eff}} = \frac{1}{4}(\sigma_1 + \sigma_2 + \sigma_3 + \sigma_4). \tag{2}$$

In what is to follow, this standard way of calculating the effective material parameters is called the E-cell method.

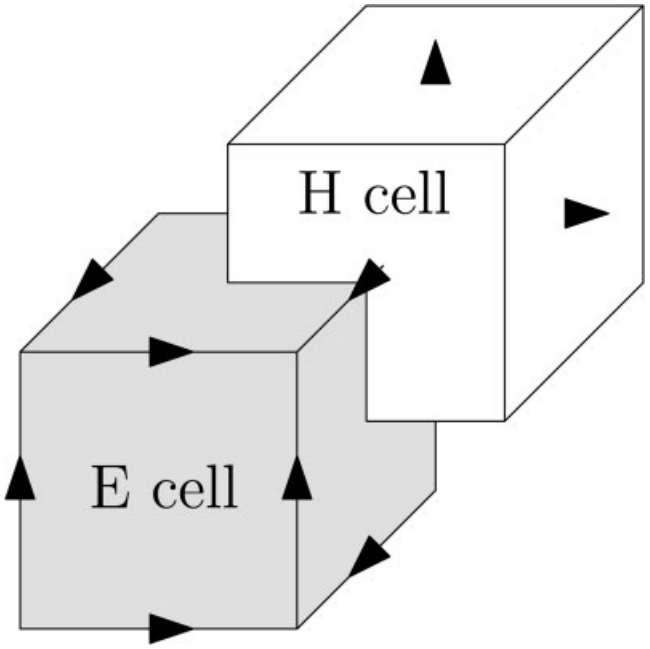


**Figure 1** Positioning of the electric field components in the E-cell and H-cell grids

An alternative to the usual E-cell method is to position the materials in the secondary grid, that is, the H-cell grid, such that the electric field components are located on the cell faces (see Fig. 1). As the electric field components are orthogonal to the boundaries of different dielectric media, it is more appropriate to speak about nonphysical effective electric field. The effective electric field is closely related to total current density (including both conductivity and displacement current), the normal component of which is continuous. Using this approach, the discontinuity condition of the normal component of the electric field—or the continuity of the effective electric field—is enforced instead of the continuity of tangential electric field.

On a material interface as shown in Figure 3, the value of the effective electric field is defined as the linear average of the physical electric fields in each cell. Effective material parameters $\varepsilon_{\text{eff}}$ and $\sigma_{\text{eff}}$ on the face are defined, such that they link the effective electric field and the total current density by

$$\left(\sigma_1 + \varepsilon_1\frac{\partial}{\partial t}\right)E_1 = \left(\sigma_2 + \varepsilon_2\frac{\partial}{\partial t}\right)E_2 = \left(\sigma_{\text{eff}} + \varepsilon_{\text{eff}}\frac{\partial}{\partial t}\right)E_{\text{eff}}, \tag{3}$$

where $E_1$ and $E_2$ are the electric field normal components in the respective cells, and $E_{\text{eff}} = 0.5\ (E_1 + E_2)$ is the effective electric field on the H-cell face.

The values of the effective parameters on the face can be derived by temporarily assuming the fields to be time harmonic (frequency $\omega$). Now, an equivalent condition for Eq. (3) is the discontinuity of the normal component of the complex electric field, that is,

$$\hat{\varepsilon}_1 E_1 = \left(\varepsilon_1 + \frac{\sigma_1}{j\omega}\right)E_1 = \hat{\varepsilon}_{\text{eff}}E_{\text{eff}} = \left(\varepsilon_2 + \frac{\sigma_2}{j\omega}\right)E_2 = \hat{\varepsilon}_2 E_2, \tag{4}$$

where $\hat{\varepsilon}_1$ and $\hat{\varepsilon}_2$ are the complex permittivities of the two media. The effective complex permittivity is thus

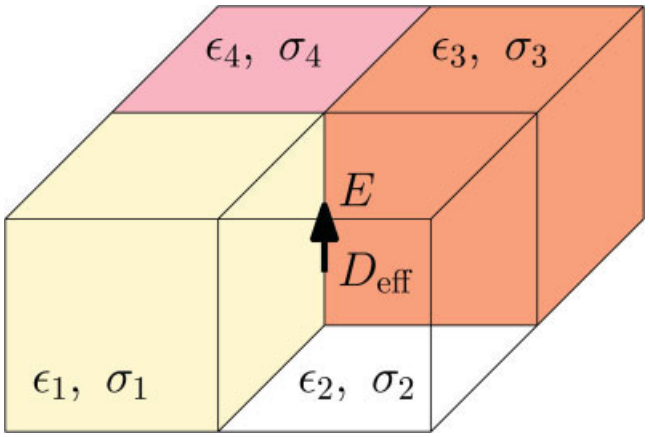


**Figure 2** Electric field component in the intersection of four E cells. [Color figure can be viewed in the online issue, which is available at www.interscience.wiley.com]

$$\hat{\varepsilon}_{\text{eff}} = \frac{2\hat{\varepsilon}_1\hat{\varepsilon}_2}{\hat{\varepsilon}_1 + \hat{\varepsilon}_2}. \tag{5}$$

The FDTD update equations require the real effective permittivity and conductivity, which are

$$\varepsilon_{\text{eff}} = \text{Re}(\hat{\varepsilon}_{\text{eff}}) = 2\frac{\varepsilon_1\sigma_2^2 + \varepsilon_2\sigma_1^2 + \omega^2\varepsilon_1\varepsilon_2(\varepsilon_1 + \varepsilon_2)}{(\sigma_1 + \sigma_2)^2 + \omega^2(\varepsilon_1 + \varepsilon_2)^2} \tag{6}$$

and

$$\sigma_{\text{eff}} = -\omega\, Im(\hat{\varepsilon}_{\text{eff}}) = 2\frac{\sigma_1\sigma_2(\sigma_1 + \sigma_2) + \omega^2(\varepsilon_1^2\sigma_1 + \varepsilon_1^2\sigma_2)}{(\sigma_1 + \sigma_2)^2 + \omega^2(\varepsilon_1 + \varepsilon_2)^2}. \tag{7}$$

The effective material parameters on the H-cell faces will generally be frequency dependent, even if the original materials are nondispersive. Naturally, modeling this dispersivity can be omitted in point-frequency simulations. In the case of nondispersive media, the high and low frequency limits for the effective permittivity and conductivity are

$$\varepsilon_{\text{eff}} \xrightarrow[\omega \to \infty]{} \frac{2\varepsilon_1\varepsilon_2}{\varepsilon_1 + \varepsilon_2} \tag{8}$$

and

$$\sigma_{\text{eff}} \xrightarrow[\omega \to 0]{} \frac{2\sigma_1\sigma_2}{\sigma_1 + \sigma_2}, \tag{9}$$

which are used in [3], in which case the normal components of both electric flux density and current density are continuous, that is, time-dependent electric charge density on dielectric interfaces is not allowed. However, for example, for human tissue interfaces at radio frequencies, these limits give values close to Eqs. (6) and (7).

Postprocessing the results of a FDTD simulation often requires the values of the physical electric field, which is not readily available on dielectric discontinuities in the H-cell case. For example, in medium 1 in Figure 3, the amplitude of the physical field can be calculated from the amplitude of the effective electric field on the face by

$$|E_1| = \left|\frac{\hat{\varepsilon}_{\text{eff}}}{\hat{\varepsilon}_1}\right||E_{\text{eff}}| = \sqrt{\frac{\omega^2\varepsilon_{\text{eff}}^2 + \sigma_{\text{eff}}^2}{\omega^2\varepsilon_1^2 + \sigma_1^2}}|E_{\text{eff}}|. \tag{10}$$

In addition to this slight difference in postprocessing, nothing but the calculation of the effective material parameters needs to be changed compared to the E-cell method. Consequently, implementing the H-cell method in an existing FDTD code is simple. Inside homogeneous media, both cell types result in exactly the same update equations, so the only difference is in the modeling of dielectric interfaces.

## 3. NUMERICAL EXAMPLES

The accuracy of both the E-cell method and the H-cell method is investigated in test simulations consisting of a sphere exposed to a linearly polarized plane wave. This setup allows comparison with the analytical Mie series solutions. Also, all simulations are performed at various FDTD cell sizes to give insight into the convergence properties of the methods. Plane-wave excitation implemented with the total-field/scattered-field technique [4] along with efficient convolution PML (CPML) absorbing boundary conditions [5] are used in the FDTD simulations. PML stands for perfectly matched layer.

### *3.1 Homogeneous Sphere*

The first test case is a lossy homogeneous sphere that is illuminated by a linearly polarized 1 V/m plane wave at 1 GHz. The permittivity and conductivity of the sphere are $\varepsilon_r = 36.5$ and $\sigma = 0.65$ S/m.

Power loss density s for each cell is determined from the amplitude of the electric field by

$$s = \frac{1}{2}\sigma\langle|E|^2\rangle = \frac{1}{2}\sigma(\langle|E_x|^2\rangle + \langle|E_y|^2\rangle + \langle|E_z|^2\rangle), \tag{11}$$

where $\langle \cdot \rangle$ means taking an average of the given quantity to the center point of the cell, and $E_x$, $E_y$, and $E_z$ are the amplitudes of the electric field components on the cell edges/faces. As seen in Figure 1, the E-cell method uses a total of twelve electric field components for averaging, while the H-cell approach needs six components. In H-cells, the electric field is calculated by Eq. (10). The required field amplitudes are calculated from the time-dependent values using the same approach as in [6].

30The average power loss density, that is, the total power loss per sphere volume, is studied for various resolutions and sphere radii.

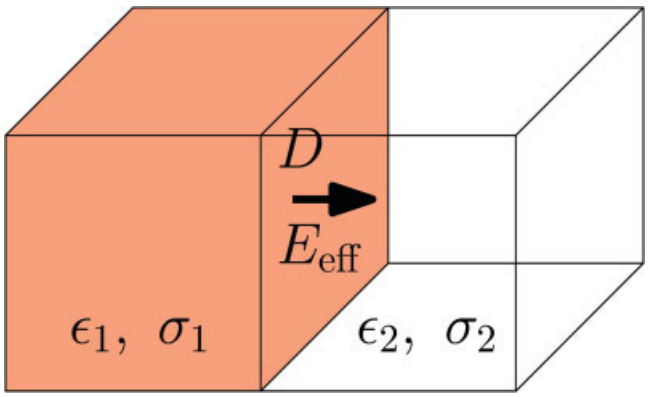


**Figure 3** Position of the electric field component on the interface of two H cells. [Color figure can be viewed in the online issue, which is available at www.interscience.wiley.com]

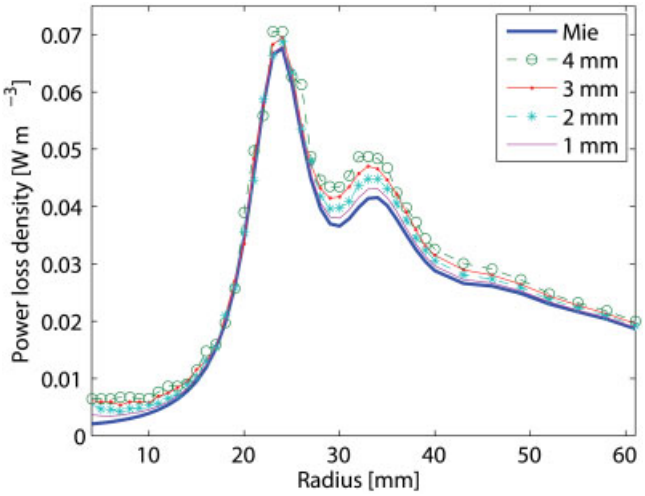


**Figure 4** Average power loss density as a function of sphere radius at various resolutions when the materials are positioned in E cells. [Color figure can be viewed in the online issue, which is available at www.interscience.wiley.com]

Plots of the average power loss density in the sphere as a function of the sphere radius are shown in Figures 4 and 5 for E cells and H cells, respectively. The two visible peaks in the figures correspond to the $TE^r$ (left peak) and $TM^r$ (right peak) sphere resonances. In the $TE^r$ resonance, electric field radial component is zero and in the $TM^r$ resonance, magnetic field radial component is zero. Interestingly, the choice of the material cell has a large effect on the accuracy of the results near these resonances. Near the $TE^r$ resonance, E cells give quite accurate results even at low resolutions, while the H cell result converges slowly with the resolution. Opposite is true for the $TM^r$ resonance. For very small spheres, E cells produce large error, while H cells seem to give reasonably accurate results.

Apparently, certain field solutions are approximated more accurately by one cell type, while the other cell type may give better results in other cases. Thus E-cell and H-cell methods seem to generally be "equally good" in terms of numerical performance.

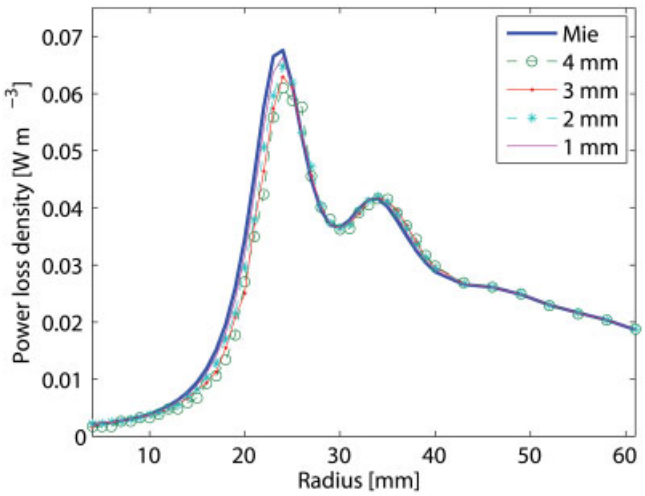


**Figure 5** Average power loss density as a function of sphere radius when the materials are positioned in H cells. [Color figure can be viewed in the online issue, which is available at www.interscience.wiley.com]

**TABLE 1 The Radii and Material Parameters of the 5-Layer Sphere**

| Tissue | Radius (mm) | $\varepsilon_r$ | $\sigma$ (S/m) |
|---|---|---|---|
| Skin | 25 | 41.0 | 0.900 |
| Fat | 21 | 5.45 | 0.054 |
| Muscle | 17 | 54.8 | 0.978 |
| Cortical bone | 13 | 12.4 | 0.156 |
| Bone marrow | 5 | 5.48 | 0.043 |

### *3.2 Layered Sphere*

Second example is a small 5-layered sphere, the materials and outer radii of which are presented in Table 1. The material parameters are assumed to be independent of the frequency (unrealistically).

Amplitude of the electric field is studied along the sphere diagonal in the plane-wave propagating direction. The amplitude in each FDTD cell is calculated by

$$|E| = \sqrt{\langle |E_x|^2 \rangle + \langle |E_y|^2 \rangle + \langle |E_z|^2 \rangle}, \tag{12}$$

where the averages are taken as in Eq. (11). Figures 6 and 7 show the electric field for two resolutions at frequencies 1 and 2.5 GHz, respectively. In the 1-GHz case, E-cell method gives slightly better agreement with the Mie theory results. But when the frequency is 2.5 GHz, the H-cell method is clearly more accurate. These results suggest that the conclusions of the previous example also hold for local fields and nonhomogeneous problems.

The H-cell simulations were also performed when the approximate formulas (8) and (9) were used. In that case, the local error in electric field values—compared to the case of the more accurate formulas (6) and (7)—was extremely small, less than 0.3% at 2-mm resolution, and even smaller for the 0.5-mm resolution.

## 4. CONCLUSIONS

An alternative H-cell method for modeling dielectric discontinuities in FDTD was proposed, and its performance was tested in numerical examples. In the H-cell method, the location of the electric field components in the FDTD grid is changed from material cell edges to faces, such that the continuity of the normal component of electric current density—including both conductiv-

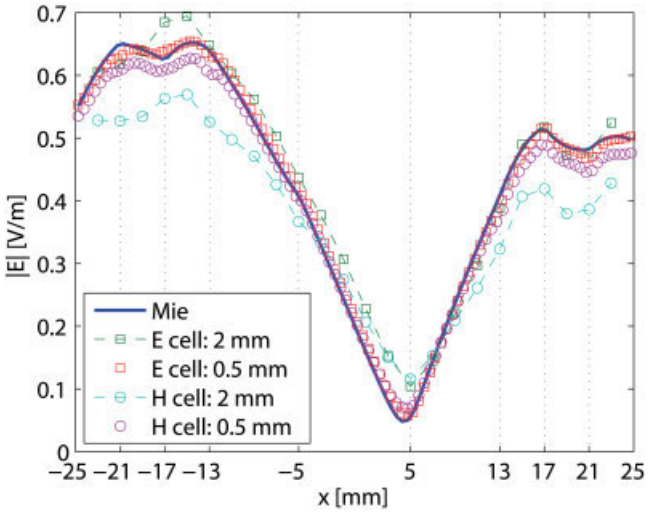


**Figure 6** Electric field amplitude along the diagonal of the 5-layer sphere at 1 GHz. [Color figure can be viewed in the online issue, which is available at www.interscience.wiley.com]

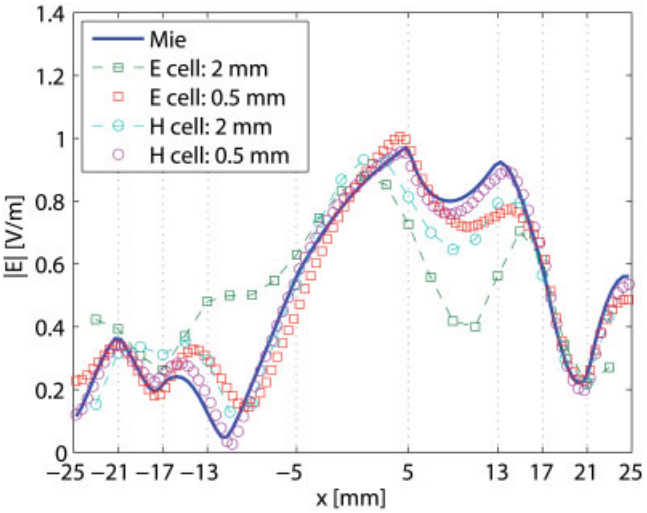


**Figure 7** Electric field amplitude along the diagonal of the 5-layer sphere at 2.5 GHz. [Color figure can be viewed in the online issue, which is available at www.interscience.wiley.com]

ity and displacement current—is enforced instead of the continuity of electric field tangential component. In the implementation of the H-cell method, the calculation of the effective material parameters on material interfaces is different compared to the standard E-cell method. Additionally, as the electric field of the FDTD simulation is not the same as the actual physical field, some simple modifications in postprocessing are needed. For example, the calculation of the electric field amplitude—or the power loss density—is altered slightly.

In terms of numerical accuracy, H-cell method is comparable with the usual E-cell method. In some cases, the proposed method may give a significant accuracy improvement, while sometimes the standard method is a better choice. Generally, the actual field solution determines which cell type gives more accurate results, which is clearly seen, for example, near the lowest $TE^r$ and $TM^r$ resonances of a dielectric sphere. For the application of the H-cell method in the field analysis inside a realistic human body model, see [6].

H-cell method can be applied to the case of magnetic dielectric materials, which allows placing the magnetic and dielectric materials in the same cells. Previously, for example, in [2], they have been positioned in separate grids; magnetic materials in the H-cell grid and dielectric materials in the E-cell grid.

## REFERENCES

1. A. Taflove and S.C. Hagness, Computational electrodynamics: The finite-difference time-domain method, 3rd ed., Artech House, Norwood, MA, 2005.
2. K.S. Kunz and R.J. Luebbers, The finite difference time domain method for electromagnetics, CRC Press, Boca Raton, FL, 1993.
3. G. Marrocco, F. Bardati, and M. Sabbadini, Field interpolation across discontinuities in FDTD, IEEE Microwave Guid Wave Lett 5 (1998), 1–3.
4. D.E. Merewether, R. Fisher, and F.W. Smith, On implementing a numeric Huygens source scheme in a finite differences program to illuminate scattering bodies, IEEE Trans Nucl Sci 27 (1980), 1829–1833.
5. J.A. Roden and S.D. Gedney, Convolution PML (CPML): An efficient FDTD implementation of the CFS-PML for arbitrary media, Microwave Opt Technol Lett 27 (2000), 334–339.
6. T. Uusitupa, S. Ilvonen, I. Laakso, and K. Nikoskinen, The effect of FDTD resolution and power-loss computation method on SAR values in plane-wave exposure of Zubal phantom, Phys Med Biol, in press.